



Universiteit
Leiden
The Netherlands

The positive effect of selective prostaglandin E2 receptor EP2 and EP4 blockade on cystogenesis in vitro is counteracted by increased kidney inflammation in vivo

Lannoy, M.; Valluru, M.K.; Chang, L.J.; Abdela-Ali, F.; Peters, D.J.M.; Streets, A.J.; Ong, A.C.M.

Citation

Lannoy, M., Valluru, M. K., Chang, L. J., Abdela-Ali, F., Peters, D. J. M., Streets, A. J., & Ong, A. C. M. (2020). The positive effect of selective prostaglandin E2 receptor EP2 and EP4 blockade on cystogenesis in vitro is counteracted by increased kidney inflammation in vivo. *Kidney International*, 98(2), 404-419. doi:10.1016/j.kint.2020.02.012

Version: Publisher's Version
License: [Creative Commons CC BY 4.0 license](#)
Downloaded from: <https://hdl.handle.net/1887/3184595>

Note: To cite this publication please use the final published version (if applicable).



The positive effect of selective prostaglandin E₂ receptor EP2 and EP4 blockade on cystogenesis *in vitro* is counteracted by increased kidney inflammation *in vivo*

Morgane Lannoy^{1,2}, Manoj K. Valluru^{1,2}, Lijun Chang^{1,2}, Fatima Abdela-Ali^{1,2}, Dorien J.M. Peters³, Andrew J. Streets^{1,2} and Albert C.M. Ong^{1,2}

¹Kidney Genetics Group, Academic Nephrology Unit, University of Sheffield Medical School, Sheffield, UK; ²Department of Infection, Immunity and Cardiovascular Disease, University of Sheffield Medical School, Sheffield, UK; and ³Department of Human Genetics, Leiden University Medical Center (LUMC), Leiden, The Netherlands

Autosomal Dominant Polycystic Kidney Disease (ADPKD) is a major cause of end-stage kidney disease in man. The central role of cyclic adenosine monophosphate (cAMP) in ADPKD pathogenesis has been confirmed by numerous studies including positive clinical trial data. Here, we investigated the potential role of another major regulator of renal cAMP, prostaglandin E₂ (PGE₂), in modifying disease progression in ADPKD models using selective receptor modulators to all four PGE₂ receptor subtypes (EP1–4). In 3D-culture model systems utilizing dog (MDCK) and patient-derived (UCL93, OX161-C1) kidney cell lines, PGE₂ strikingly promoted cystogenesis and inhibited tubulogenesis by stimulating proliferation while reducing apoptosis. The effect of PGE₂ on tubulogenesis and cystogenesis in 3D-culture was mimicked or abolished by selective EP2 and EP4 agonists or antagonists but not those specific to EP1 or EP3. In a *Pkd1* mouse model (*Pkd1*^{nl/nl}), kidney PGE₂ and COX-2 expression were increased by two-fold at the peak of disease (week four). However, *Pkd1*^{nl/nl} mice treated with selective EP2 (PF-04418948) or EP4 (ONO-AE3-208) antagonists from birth for three weeks had more severe cystic disease and fibrosis associated with increased cell proliferation and macrophage infiltration. A similar effect was observed for the EP4 antagonist ONO-AE3-208 in a second *Pkd1* model (*Pax8rtTA-TetO-Cre-Pkd1*^{fl/fl}). Thus, despite the positive effects of slowing cyst growth *in vitro*, the more complex effects of inhibiting EP2 or EP4 *in vivo* resulted in a worse outcome, possibly related to unexpected pro-inflammatory effects.

Kidney International (2020) 98, 404–419; <https://doi.org/10.1016/j.kint.2020.02.012>

KEYWORDS: ADPKD; cyclic AMP; cystogenesis; inflammation; macrophages; prostaglandin E₂

Copyright © 2020, International Society of Nephrology. Published by Elsevier Inc. All rights reserved.

Correspondence: Albert Ong, Academic Nephrology Unit, Department of Infection, Immunity and Cardiovascular Disease, University of Sheffield, Medical School, Beech Hill Road, Sheffield S10 2RX, UK. E-mail: a.ong@sheffield.ac.uk

Received 2 January 2019; revised 16 January 2020; accepted 7 February 2020; published online 6 March 2020

Translational Statement

Autosomal dominant polycystic kidney disease (ADPKD), which currently has limited treatment options, is the major genetic cause of kidney failure in humans. Our study sought to investigate whether selective receptor blockade of prostaglandin E₂ action via the EP2 and EP4 receptors, which signal mainly via cyclic adenosine monophosphate, could inhibit cyst formation in experimental disease models. Despite positive effects in cyst assays, an unexpected increase in the cyst burden was observed in 2 *Pkd1* mouse models after *in vivo* dosing, associated with an increase in inflammation. Our results do not support the use of EP2 or EP4 antagonists as therapeutic options in ADPKD.

Autosomal dominant polycystic kidney disease (ADPKD) is the most common kidney genetic disorder, accounting for 7%–10% of patients with end-stage renal disease, and is caused by mutations in 1 of 2 genes, *PKD1* (~85%) and *PKD2* (~15%).¹ It is characterized by the formation of fluid-filled cysts that arise from tubular epithelial cells that exhibit a hyperproliferative and pro-apoptotic phenotype.^{2,3} Recently, the vasopressin V2 receptor (VPV2R) antagonist tolvaptan has been approved for treatment of ADPKD patients who show evidence of rapid disease progression.^{4,5} However, the use of tolvaptan is associated with poorly tolerated side effects and a rare but unpredictable incidence of liver toxicity.⁴ Hence, the discovery of safer and more effective alternative drugs to slow disease progression in ADPKD is of major clinical interest.

Prostaglandin E₂ (PGE₂) is a lipid mediator synthesized from arachidonic acid through several enzymatic steps including production of cyclooxygenases (COX-1 and COX-2) and prostaglandin synthase.⁶ Several studies suggest that COX-2 is the major cyclooxygenase responsible for PGE₂ production.^{7,8} PGE₂ binds to 4 different G-protein-coupled receptors (GPCRs)—prostaglandin E₂ receptors 1–4 (EP1–4)—which are differentially expressed in different tissues and

signal through different G-proteins, resulting in complex outputs.⁹ In particular, EP2 and EP4 are known to couple to G_s, which stimulates cyclic adenosine monophosphate (cAMP) formation by activating adenylyl cyclase.¹⁰ Cyclic AMP is a central player in cyst formation and expansion.^{11–14} Several GPCR ligands (vasopressin V2 receptor [VPV2R], endothelin B, and somatostatin receptors) have been shown to modify disease severity in ADPKD models through modulation of renal cAMP concentrations.^{15–18}

PGE₂ has been isolated in cyst fluid,¹⁹ and its urinary concentration has been found to be increased in patients with reduced kidney function.²⁰ *In vitro*, the effect of PGE₂ on stimulating cyst formation has been shown on inner medullary collecting duct (IMCD)-3 and human epithelial cells.^{21,22} These early observations suggested that PGE₂ could be a major modifier of cyst growth. However, the study of PGE₂ signalling has been hampered by the lack of potent and selective receptor modulators (agonists and antagonists). Conversely, the more recent availability of these compounds has led to a resurgence of preclinical and clinical investigation of different EP subtypes as selective targets to treat a variety of orphan diseases.²³

In this article, we report the effects of modifying PGE₂ signalling on cyst growth by utilizing new potent and selective receptor modulators of all 4 EP receptors (EP1–4) in cellular and animal models of ADPKD. Our results suggest a striking effect of EP2 and EP4 agonists in inhibiting tubulogenesis and promoting cyst formation and expansion *in vitro*. However, the administration of EP2 and EP4 antagonists to a neonatal model of ADPKD, the hypomorphic *Pkd1*-neolox mouse (*Pkd1*^{nl/nl}) and a postnatal Cre-inducible *Pkd1* model (*Pax8*^{rtTA}-*TetO-Cre-Pkd1*^{fl/fl}), led, surprisingly, to more severe cystic disease. These results suggest a more complex effect of EP2 and EP4 antagonists *in vivo*, resulting in a worse outcome in this model, possibly related to unexpected proinflammatory effects.

RESULTS

EP2 and EP4 receptor activation inhibits tubulogenesis and promotes cystogenesis

To study the effect of PGE₂ on spontaneous tubulogenesis, the normal human renal epithelial cell line UCL93 was grown in a Type I collagen matrix. After 20 days, prominent tubule structures had formed with evidence of branching (Figure 1a). The addition of different concentrations of PGE₂ (1–100 nM) after 6 days of culture significantly increased the percentage of cystic structures, with a 2-fold increase at 10 nM PGE₂ (Figure 1b). All 4 EP receptor subtypes are expressed in this line, although EP2 and EP4 were more highly expressed than EP1 and EP3 (data not shown). The effect of PGE₂ was mimicked by an EP2 selective agonist (ONO-AE1-259-01) and by an EP4 selective agonist (ONO-AE1-329), suggesting that stimulation of either receptor can initiate cyst formation (Figure 1c and d). Stimulation of UCL93 with PGE₂, EP2, or EP4 selective agonists stimulated cAMP formation (Figure 1e and f), suggesting that cyst formation is cAMP-mediated and involves EP2 and EP4.

PGE₂ stimulates cyst growth in Madin-Darby canine kidney cell (MDCK) and OX161-C1 cell lines

The potential effect of PGE₂ and its receptors on cyst growth was next studied in 3D-cyst assays using the established MDCK II, and in a human *PKD1* cystic epithelial cell line, OX161-C1 (Figure 2a). The latter expresses all 4 EP subtypes in a pattern similar to that of UCL93 (data not shown). The addition of PGE₂ significantly enhanced cyst growth in both cell lines over time in a dose-dependent manner, with OX161-C1 cells being more sensitive than MDCK II cells to the effect of PGE₂ (Figure 2b and c). Given that MDCK II cysts responded in a clearer dosage-dependent manner than OX161-C1, we investigated the effects of PGE₂ on proliferation (antigen Ki-67) or apoptotic (cleaved caspase-3) rates in MDCK II cysts. PGE₂ had a dual effect on MDCK II cysts, both increasing cell proliferation and inhibiting apoptosis in a dose-dependent manner (Figure 2d–g). We did not measure apoptosis at earlier time points and it is possible that luminal apoptotic cells could have been removed. These changes were significantly correlated to changes in the average cyst area measured in the same wells (Supplementary Figure S1A and B). As expected, PGE₂ stimulated cAMP accumulation in both cell lines (Supplementary Figure S1C and D).

EP2 and EP4 agonists mimic PGE₂-induced cyst growth

A differential array of EP gene expression revealed fold-changes of 1.55 (EP1), 5.05 (EP2), 1.19 (EP3), and 1.89 (EP4) between *PKD1* cystic and normal cells, although only EP2 was significantly increased.²⁴ We confirmed that OX161-C1 expresses all 4 EP receptor subtypes, and MDCK II expresses EP2 and EP4 mRNA by polymerase chain reaction (data not shown). We next tested the effects of selective agonists to EP1–4 in both cell lines grown in 3D-culture for up to 20 days. The EP1 agonist ONO-DI-004 and the EP3 agonist ONO-AE-248 did not significantly increase cyst area in either MDCK II or OX161-C1 after 14 days of incubation, although a decrease was noted at the highest concentration of ONO-AE-248 in OX161-C1 (data not shown). By contrast, cyst growth in both lines was significantly enhanced by either EP2 (ONO-AE1-259-01) or EP4 (ONO-AE1-329) agonists in a dose-dependent manner (Figure 3a–d). Similar to PGE₂, the EP2 and EP4 agonists also enhanced cAMP formation in OX161-C1 and MDCK II (Figure 3e and f) and stimulated MDCKII cyst growth by increasing cell proliferation and decreasing cell apoptosis (Supplementary Figure S2). These results strongly suggest that PGE₂ stimulates cyst growth *in vitro* by activating EP2 and EP4.

EP2 and EP4 antagonists abolish PGE₂-induced cyst growth

To confirm that PGE₂-induced cyst growth is mediated by EP2 and EP4, we tested the effect of selective EP2 and EP4 antagonists on PGE₂-induced cyst growth in both cell lines. As shown in Figure 4, the EP2 antagonist ONO-AE8-111 and the EP4 antagonist ONO-AE8-11 both decreased the effect of PGE₂ on cyst growth. Similar effects were observed with the EP2 antagonist PF-04418948 and a different EP4 antagonist

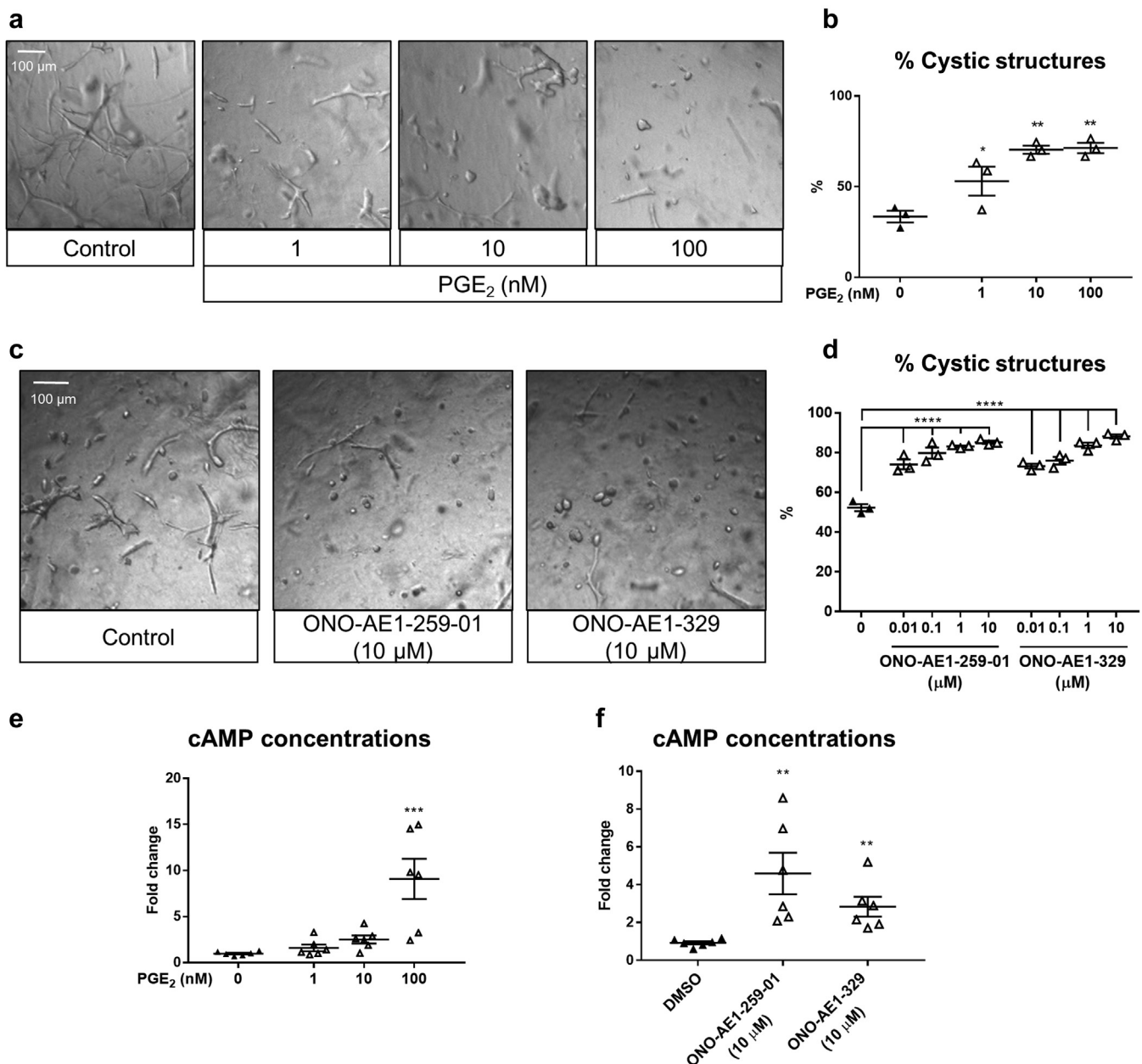


Figure 1 | Prostaglandin E2 (PGE₂) inhibits tubulogenesis and promotes cystogenesis through EP2 and EP4 receptors. (a,b) PGE₂, ONO-AE1-259-01, an EP2 receptor agonist, and (c,d) ONO-AE1-329, an EP4 receptor agonist, inhibit spontaneous tubulogenesis in UCL93, a noncystic human renal epithelial cell line, grown initially for 6 days to promote tubular formation and then incubated for a further 14 days with compounds. Bar = 500 μ m. Values are expressed as mean \pm SEM, $n > 100$ structures per condition. (e) PGE₂, ONO-AE1-259-01, and (f) ONO-AE1-329 stimulate cyclic adenosine monophosphate (cAMP) accumulation in UCL93 cells after 60 minutes of incubation. Values are expressed as mean \pm SEM, $n = 6$. * $P < 0.05$; ** $P < 0.01$; *** $P < 0.001$; **** $P < 0.0001$, compared with the control group. Statistical significance was determined using a 1-way analysis of variance followed by Dunnett's multiple comparison test or an unpaired t test. DMSO, dimethylsulfoxide.

CJ-42794 (data not shown). Taken together, these results confirm that PGE₂ induces cyst growth via EP2 and EP4 and that blockade of either receptor is sufficient to inhibit the effect of PGE₂.

The PGE₂ pathway is upregulated in an early-onset *Pkd1* mouse model

To study the regulation of the PGE₂ pathway in an *in vivo* ADPKD model, we utilized the early-onset hypomorphic

Pkd1^{nl/nl} mouse model.²⁵ In this model, *Pkd1*^{nl/nl} kidneys were already cystic and larger at birth compared to *Pkd1*-wildtype (*Pkd1*^{wt/wt}) at each time point (Supplementary Figure S3A–E). Typically, peak kidney growth and cyst expansion occurred around week 3, followed by a gradual decrease up to week 10 (Figure 5a and b; Supplementary Figure S3F). Cysts developed from multiple nephron segments (distal and proximal tubules, collecting ducts, and loop of Henle) during this growth phase (data not shown). At 3 weeks, *Pkd1*^{nl/nl} kidneys were

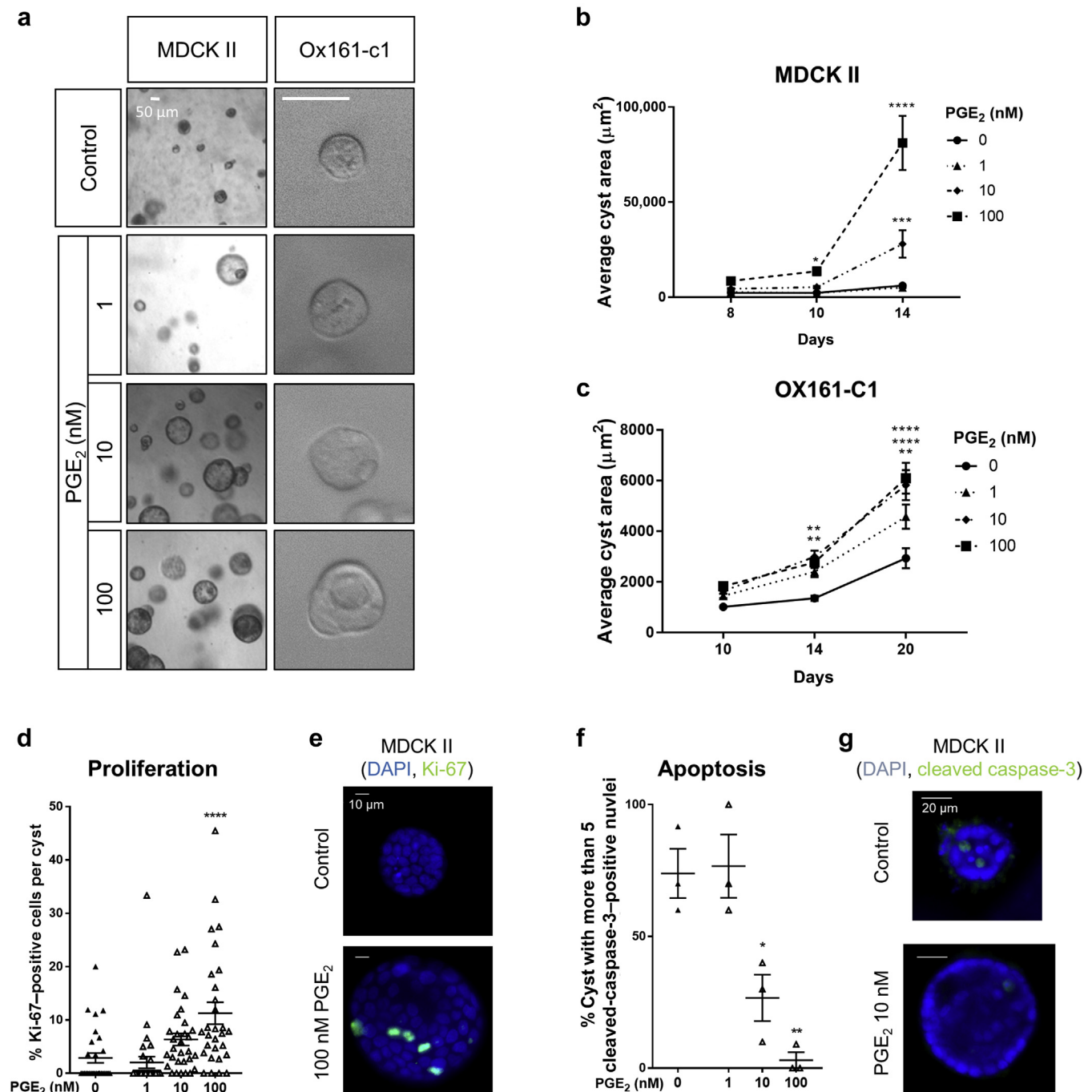


Figure 2 | Prostaglandin E₂ (PGE₂) induces cyst growth by increasing proliferation and decreasing apoptosis. (a–c) PGE₂ stimulates cyst growth in Madin-Darby canine kidney cell (MDCK) II and OX161-C1 cells in a dose- and time-dependent manner. Bar = 50 μm . Values are expressed as mean \pm SEM; $n = 30$ –78 cysts per condition for MDCK II, and $n = 84$ –113 cysts per condition for OX161-C1. * $P < 0.05$; ** $P < 0.01$; *** $P < 0.001$; **** $P < 0.0001$, compared with the control group. Statistical significance was determined using a 2-way analysis of variance followed by Tukey's multiple-comparison test. PGE₂ (d,e) stimulates cell proliferation and (f,g) inhibits apoptosis in a dose-dependent manner in MDCK II cysts. The proliferative rate at day 10 was quantified as the percentage of antigen Ki-67-positive cells per cyst. The apoptotic rate was quantified as the percentage of cysts with > 5 cleaved caspase-3-positive nuclei. Values are expressed as mean \pm SEM, $n = 30$ cysts per condition. * $P < 0.05$; ** $P < 0.01$; **** $P < 0.0001$, compared with the control group. Statistical significance was determined using a 1-way analysis of variance followed by Dunnett's multiple-comparison test. DAPI, 4',6-diamidino-2-phenylindole. To optimize viewing of this image, please see the online version of this article at www.kidney-international.org.

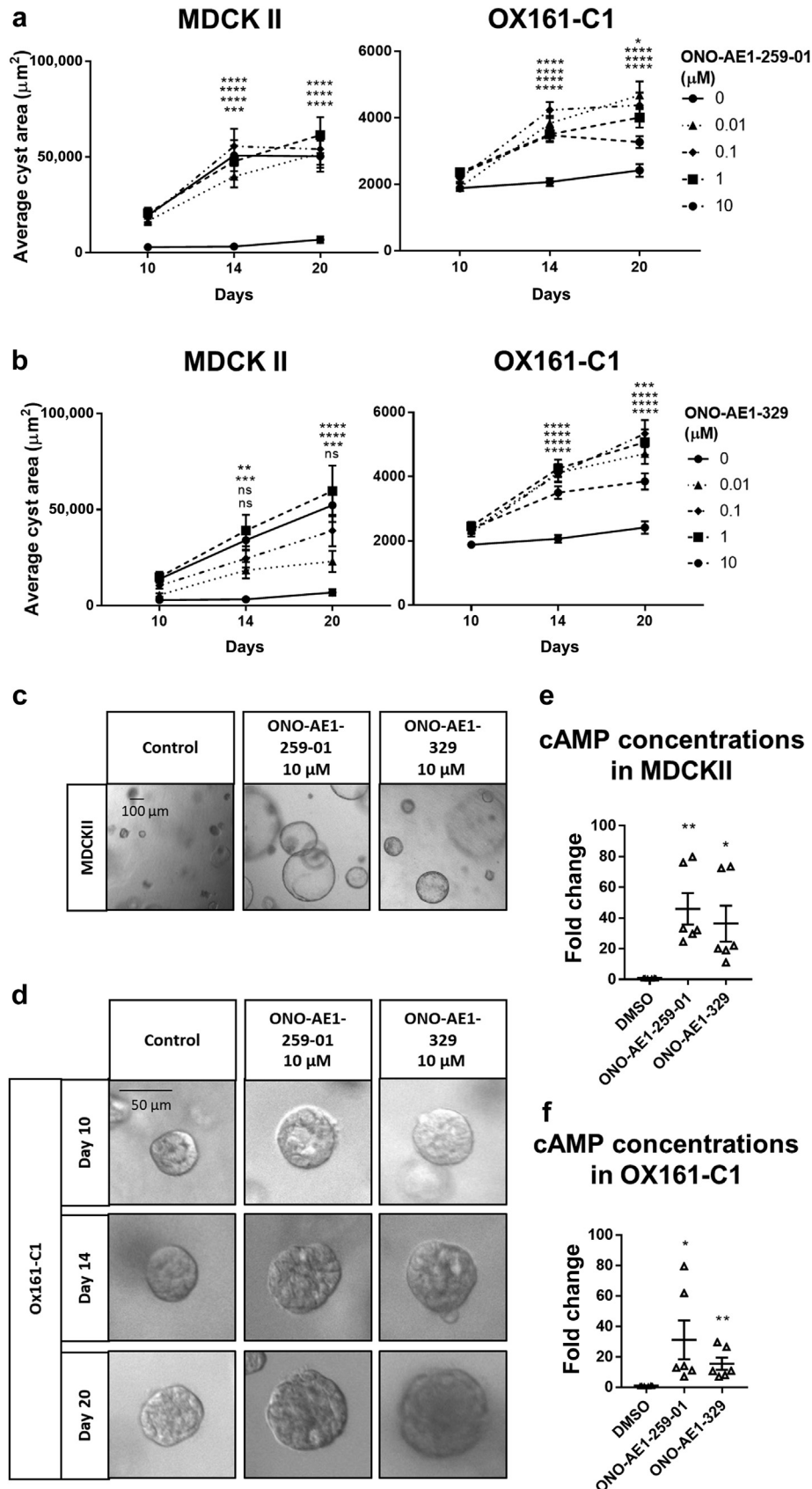


Figure 3 | Prostaglandin E receptor (EP)2 and EP4 activation induce cyst growth of Madin-Darby canine kidney cell (MDCK) II and OX161-C1 cells. The (a) EP2 receptor agonist ONO-AE1-259-01 and (b) the EP4 receptor agonist ONO-AE1-329 stimulated cyst growth in (continued)

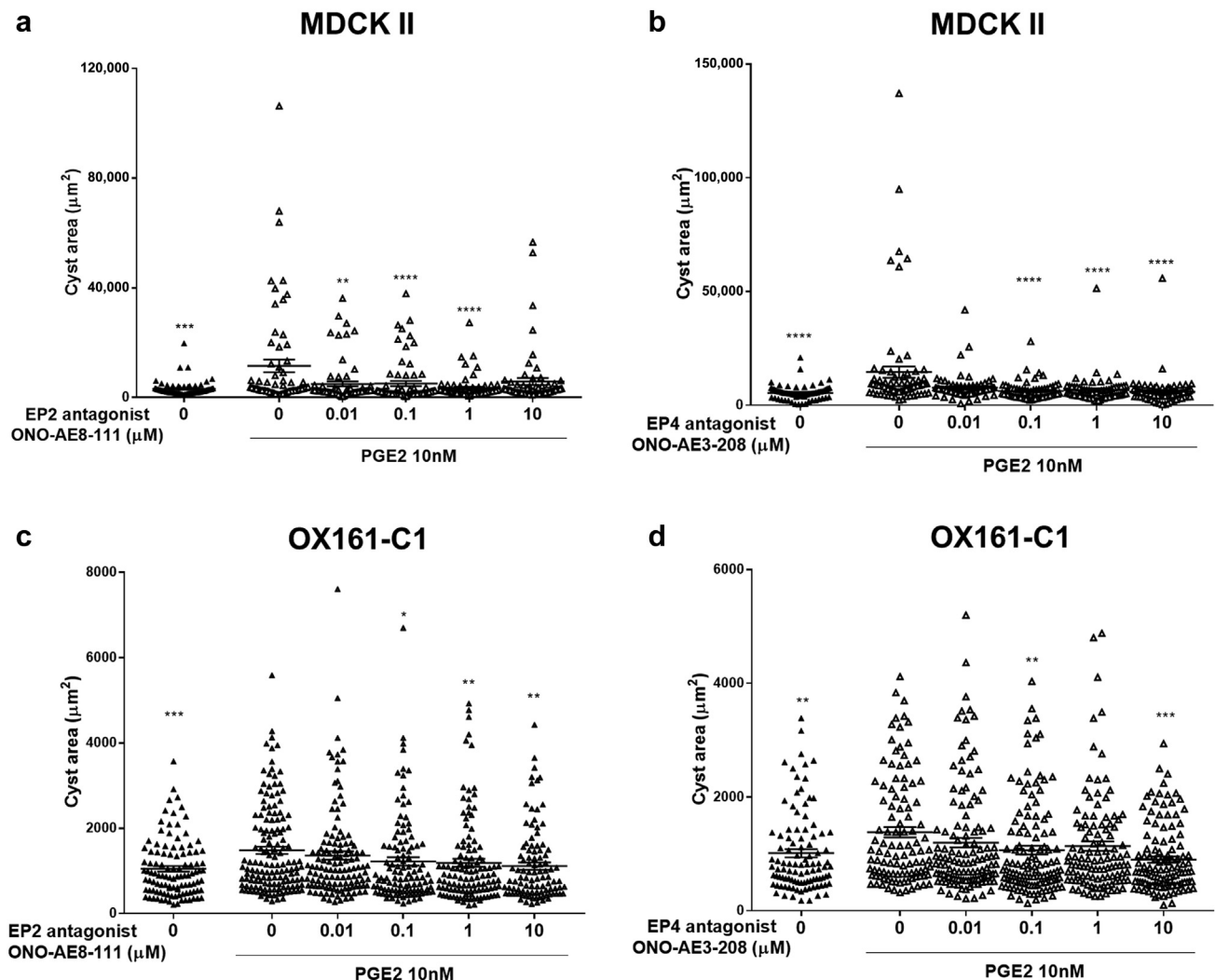


Figure 4 | Prostaglandin E receptor (EP)2 and EP4 antagonists abolish prostaglandin E₂ (PGE₂)-induced cyst growth *in vitro*. The effect of PGE₂ (10 nM) on cyst growth in (a,b) Madin-Darby canine kidney (MDCK) II and (c,d) OX161-C1 cells is blocked by EP2 (ONO-AE8-111) or EP4 (ONO-AE3-208) selective antagonists after 14 days and 10 days, respectively. Values are expressed as mean \pm SEM, $n = 64$ –75 cysts per condition for MDCK II, and $n = 101$ –144 cysts per condition for OX161-C1. * $P < 0.05$; ** $P < 0.01$; *** $P < 0.001$; **** $P < 0.0001$, compared with the PGE₂ group (■). Statistical significance was determined using the nonparametric Kruskal-Wallis test followed by a Dunn's multiple-comparisons test.

characterized by an increase in both proliferative (Ki-67-positive) and apoptotic (dUTP nick-end labeling [TUNEL]-positive) cells (Supplementary Figure S4), an accumulation of F4/80-positive cells, and fibrotic tissue especially around cysts (Supplementary Figure S5). Renal cAMP concentrations increased significantly from week 2 to 3 in *Pkd1^{nl/nl}* kidneys but then decreased sharply after

week 4, changing in parallel to fractional total kidney weights (Figure 5a and c).

We next analyzed different components of the PGE₂ system in this model. Levels of *Ptgs2* mRNA (encoding for COX-2) were increased in *Pkd1^{nl/nl}* kidneys from weeks 2 to 6, followed by a decline up to week 10 (Figure 5d). In 4-week-old animals, PGE₂ concentrations in whole kidney lysates was

Figure 3 | (continued) MDCK II and OX161-C1 cells. Values are expressed as mean \pm SEM, $n = 45$ –72 cysts per condition for MDCK II, and $n = 73$ –162 cysts per condition for OX161-C1. * $P < 0.05$; ** $P < 0.01$; *** $P < 0.001$; **** $P < 0.0001$, compared with the control group. Statistical significance was determined using a 2-way analysis of variance followed by Tukey's multiple-comparison test. (c) Example of MDCKII cysts after 20 days of ONO-AE1-259-01 or ONO-AE1-329. Bar = 100 μm . (d) Example of OX161-C1 cysts after 10, 14, and 20 days of incubation with ONO-AE1-259-01 or ONO-AE1-329. Bar = 50 μm . ONO-AE1-259-01 or ONO-AE1-329 stimulate cyclic adenosine monophosphate (cAMP) accumulation in (e) MDCK II and (f) OX161-C1 cells after 60 minutes. Values are expressed as mean \pm SEM, $n = 6$. * $P < 0.05$; ** $P < 0.01$, compared with the control group. Statistical significance was determined using a 1-way analysis of variance followed by Dunnett's multiple-comparison test or an unpaired *t* test. DMSO, dimethylsulfoxide.

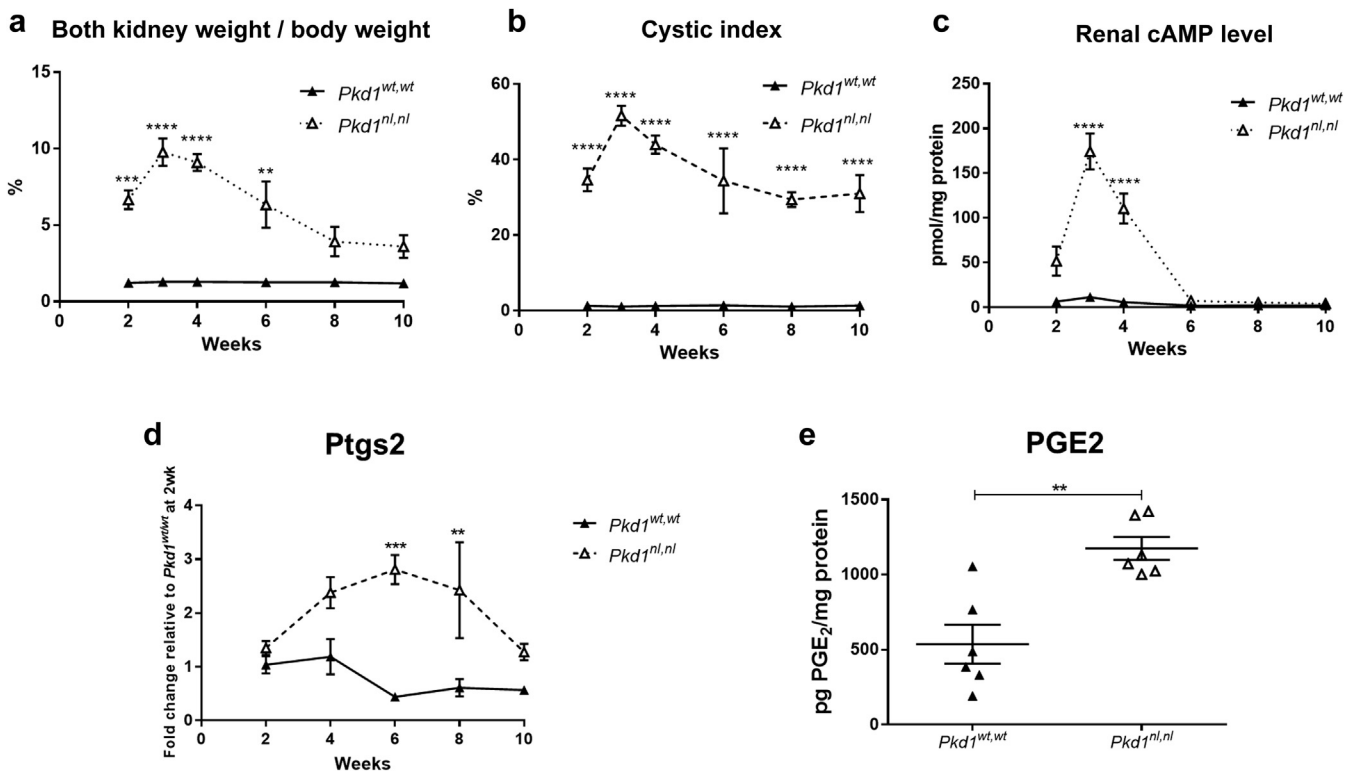


Figure 5 | The evolution of cystic disease in *Pkd1*^{nl/nl} mice is associated with an upregulation of prostaglandin E₂ (PGE₂) synthesis. Measurements were taken of (a) kidney-to-body weight ratio, (b) cystic index, (c) renal cyclic adenosine monophosphate (cAMP) content, and (d) *Ptgs2* mRNA in *Pkd1*^{wt,wt} and *Pkd1*^{nl,nl} kidneys from PN14 to PN70. Values are expressed as mean ± SEM (*n* = 4–11 per group). ***P* < 0.01; ****P* < 0.001, *****P* < 0.0001, compared to *Pkd1*^{wt,wt} at the same age. Statistical significance was determined using a 2-way analysis of variance followed by Tukey's multiple-comparison test. (e) PGE₂ concentrations were measured on whole kidney lysates from 4-week-old *Pkd1*^{wt,wt} and *Pkd1*^{nl,nl}. Values are expressed as mean ± SEM (*n* = 6 per group). ***P* < 0.01 compared to *Pkd1*^{wt,wt}. Statistical significance was determined using an unpaired *t* test.

increased by at least 2-fold: 537 pg/mg protein (*Pkd1*^{wtwt}) versus 1174 pg/mg protein (*Pkd1*^{nl/nl}; Figure 5e). The expression profile of the different PGE₂ receptors showed distinct expression patterns over time (Supplementary Figure S6). *Ptger1* and *Ptger4* mRNA were significantly upregulated in *Pkd1*^{nl/nl} kidney from weeks 4 to 10, with a peak at week 6, whereas *Ptger2* was significantly upregulated at week 2 and also from weeks 6 to 10. *Ptger3* expression was lower in *Pkd1*^{nl/nl} kidneys between weeks 2 to 6, although this change was not statistically significant. In 2-week-old *Pkd1*^{wtwt} kidneys, EP4 was strongly expressed by distal tubules and the loops of Henle, colocalizing with calbindin and Tamm-Horsfall protein, respectively, in serial sections (Supplementary Figure S7A). In 2-week-old *Pkd1*^{nl/nl} kidneys, EP4 was detected in small cysts and dilated tubules but was not expressed in larger cysts (Supplementary Figure S7B). Unfortunately, we did not find an EP2 antibody suitable for immunohistochemistry.

EP2 and EP4 receptor blockade increases disease severity *in vivo* in an early-onset *Pkd1* mouse model

Given that cyst formation occurred *in utero* and was obvious in newborn (postnatal day [PN]1) *Pkd1*^{nl/nl} mice (Supplementary Figure S3), we decided to commence drug

treatment shortly after birth. To achieve this, compounds were initially administered through the drinking water (PN1–7) of lactating mothers and after the first week of life, by daily i.p. injection (PN7–20) to the pups. Four treatment groups each received either dimethylsulfoxide (vehicle), the EP2 antagonist PF-04418948, the EP4 antagonist ONO-AE3-208, or both compounds in combination (Figure 6a). Animals from all 4 groups grew normally and tolerated the compounds with normal increases in body weight (data not shown). Unexpectedly, the average kidney weights and kidney-to-body weight ratio from PN21 mice treated with either EP2 or EP4 antagonists alone did not decrease but rather were higher (Figure 6b–d), with a significant increase for the EP4 antagonist-treated animals. Histologic analysis of kidney sections showed that the cystic index in both the EP2- and EP4-treated groups were significantly higher than those of vehicle-treated animals (Figure 6e and f), with a nonsignificant trend (*P* = 0.056) toward increased fibrosis (Supplementary Figure S8D). Kidney function was not significantly altered between the groups, nor was there a significant change in total kidney cAMP content or apoptosis (Supplementary Figure S8A–C). However, the percentage of Ki-67-positive cells and F4/80-positive cells was significantly increased in both the EP2 and EP4 groups,

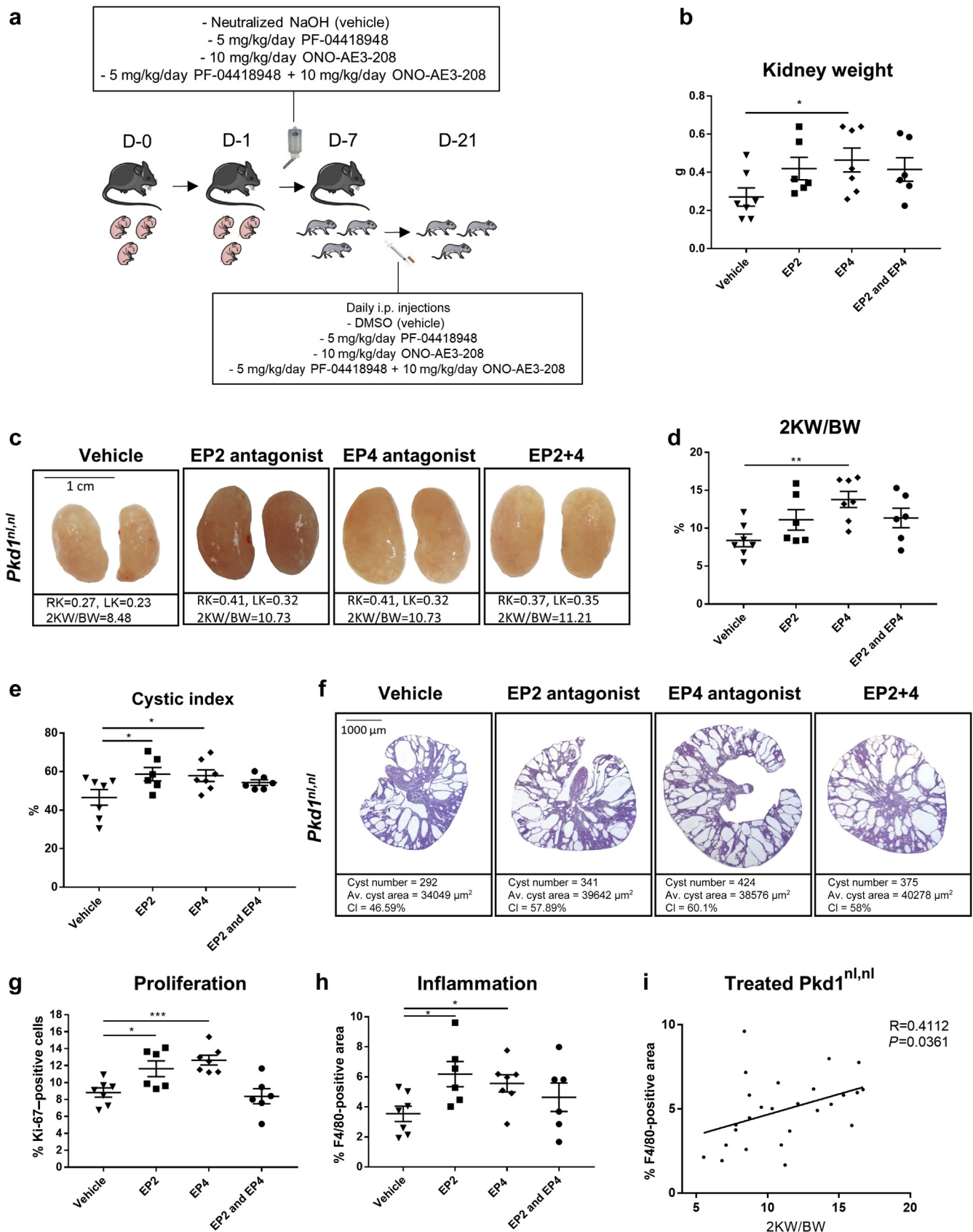


Figure 6 | Administration of prostaglandin E receptor (EP2) and EP4 antagonists worsened the cystic phenotype of *Pkd1*^{nl,nl} mice. (a) Outline of the experimental design of the *in vivo* experiments. **(b)** Kidney weights of PN21 *Pkd1*^{nl,nl} mice treated with EP2 or EP4 (continued)

with a significant correlation between the percentage of F4/80-positive cells and the kidney-to-body weight ratio (Figure 6g–i). Compared to vehicle-treated animals, mice treated with EP2 and EP4 antagonists in combination had a less severe phenotype than those treated with either compound alone, associated with a trend toward reduced fibrosis, cell proliferation, and macrophage number. Treated animals did not show any significant change between aquaporin (AQP)1- and AQP2-positive tubules, excluding a differential effect on segment-specific cysts (Supplementary Figure S9).

EP4 receptor blockade *in vivo* increases disease severity in an inducible kidney-specific *Pkd1* model

To confirm these findings, we utilized a second *Pkd1* mouse model (*Pax8^{rtTA}-TetO-Cre-Pkd1^{fl/fl}*)²⁶ to induce kidney-specific post-natal *Pkd1* deletion (PN13–15) by doxycycline (DOX) i.p. injection, which generates a less severe model than *Pkd1^{nl/nl}* mice. Postinduction, mice were treated by daily i.p. injection for 14 days (PN16–29) prior to sacrifice at PN30. The 4 treatment groups received either dimethylsulfoxide (vehicle), the EP2 antagonist PF-04418948, the EP4 antagonist ONOAE3-208, or both compounds in combination (Figure 7a). Average kidney weights and kidney-to-body weight ratios treated with the EP4 antagonist were higher than vehicle- or EP2-treated mice, with a nonsignificant increase in the EP4 antagonist-treated animals (Figure 7b–d). Although there was no significant change in cystic index, cyst number in the EP4-treated group was higher ($P = 0.053$) than in vehicle-treated animals (Figure 7e–g) and was associated with a significant increase in the percentage of Ki-67-positive cells and F4/80-positive cells (Figure 7h and i). As in the first model (*Pkd1^{nl/nl}*), the percentage of F4/80-positive cells and the kidney-to-body weight ratio showed a highly significant correlation (Figure 7j).

EP4 receptor blockade *in vivo* increases accumulation of M2 macrophages in both *Pkd1* models

The observed increase in macrophage number, particularly following EP4 receptor blockade, led us to investigate whether there was a shift in macrophage polarization between M1 (Nos2-positive) and M2 (Ym1- or Mrc1-positive) subtypes by immunohistochemistry and immunofluorescence labelling. In both models, M2 macrophages (Ym1 or Mrc1) were significantly increased in the EP4 group (Figure 8), whereas the percentage of M1 macrophages did not change (Supplementary Figure S10).

DISCUSSION

In this study, we present clear evidence that PGE₂ promotes cystogenesis in cellular models of ADPKD via the EP2 and EP4 receptors. Given that EP2 and EP4 are known to couple to Gs, which stimulates cAMP formation by activating adenylyl cyclase,^{27,28} this confirms that the pro-cystogenic action of PGE₂ occurs *via* cAMP formation. Using selective receptor agonists, we exclude a major role for EP3, which inhibits cAMP generation *via* Gi²⁹ and EP1, which activates Gq, leading to intracellular Ca²⁺ elevation through phospholipase C.³⁰ The effect of PGE₂ acting via EP2 and EP4 was particularly striking on inhibiting normal tubulogenesis and promoting cystogenesis in a non-cystic human cell line (UCL93). The action of EP2 and EP4 appeared to be independent and nonredundant in both MDCK and OX161-C1. We did not observe a change in the pattern of EP receptor expression between normal (UCL93) versus PKD1 cystic cells. Our results differ from previous reports suggesting a more restricted role for EP2 and EP4 in mediating the action of PGE₂ on cyst formation in primary human cystic cells and murine IMCD-3 cells, respectively.^{21,22} These differences could reflect cell-type differences in EP expression.

The promising effects observed using EP2 and EP4 antagonists on PGE₂-induced cyst growth *in vitro* were, however, not reproduced *in vivo*. We chose to study a well-established *Pkd1* mouse model (*Pkd1^{nl/nl}*), which has an early-onset phenotype but whose phenotype has been shown to respond to several therapeutic drugs.^{31–34} Both PGE₂ concentration and *Ptgs2* expression were increased at the peak of cystic disease (3–4 weeks) in parallel to the increase in renal cAMP concentrations. Given that cyst formation was already significant at birth, we decided to administer EP2 and EP4 antagonists from PN1–21 to cover the peak period of cyst formation. Unexpectedly, blockade of either receptor led to an increase in the severity of disease and was associated with an increase in cell proliferation and macrophage infiltration. Similar results were observed for EP4 blockade in a second *Pkd1* model (*Pax8^{rtTA}-TetO-Cre-Pkd1^{fl/fl}*) with postnatal disease onset, although in this model, the effect of EP2 antagonism was neutral. These findings could represent differences relating to the timing of disease onset in both models, i.e., neonatal (hypomorphic) and postnatal (inducible).

The simplest explanation for our findings is that EP2 and EP4 antagonism led to a proinflammatory phenotype *in vivo*. Indeed, the role of PGE₂ in inflammation is complex, as it has been reported to exert both pro- and anti-inflammatory responses, depending on the tissue and

Figure 6 | (continued) antagonists. (c) Gross morphology of *Pkd1^{nl/nl}* kidneys from mice treated with EP2 or EP4 antagonists. (d) Two kidney-to-body weight ratios (2KW/BW), (e) cystic index, and (f) representative images of periodic acid–Schiff–stained kidney sections from *Pkd1^{nl/nl}* kidneys from mice treated with EP2 or EP4 antagonists. Percentage of (g) Ki-67-positive cells and (h) F4/80-positive cells in kidney sections from mice treated with EP2 or EP4 antagonists. (i) Correlation between the percentage of F4/80-positive cells and fractional kidney weights. Values are expressed as mean ± SEM ($n = 6–7$ per group). * $P < 0.05$; ** $P < 0.01$; *** $P < 0.001$, compared to vehicle group. Statistical significance was determined using an unpaired t test. Av., average; CI, confidence interval; DMSO, dimethylsulfoxide; LK, left kidney; RK, right kidney. To optimize viewing of this image, please see the online version of this article at www.kidney-international.org.

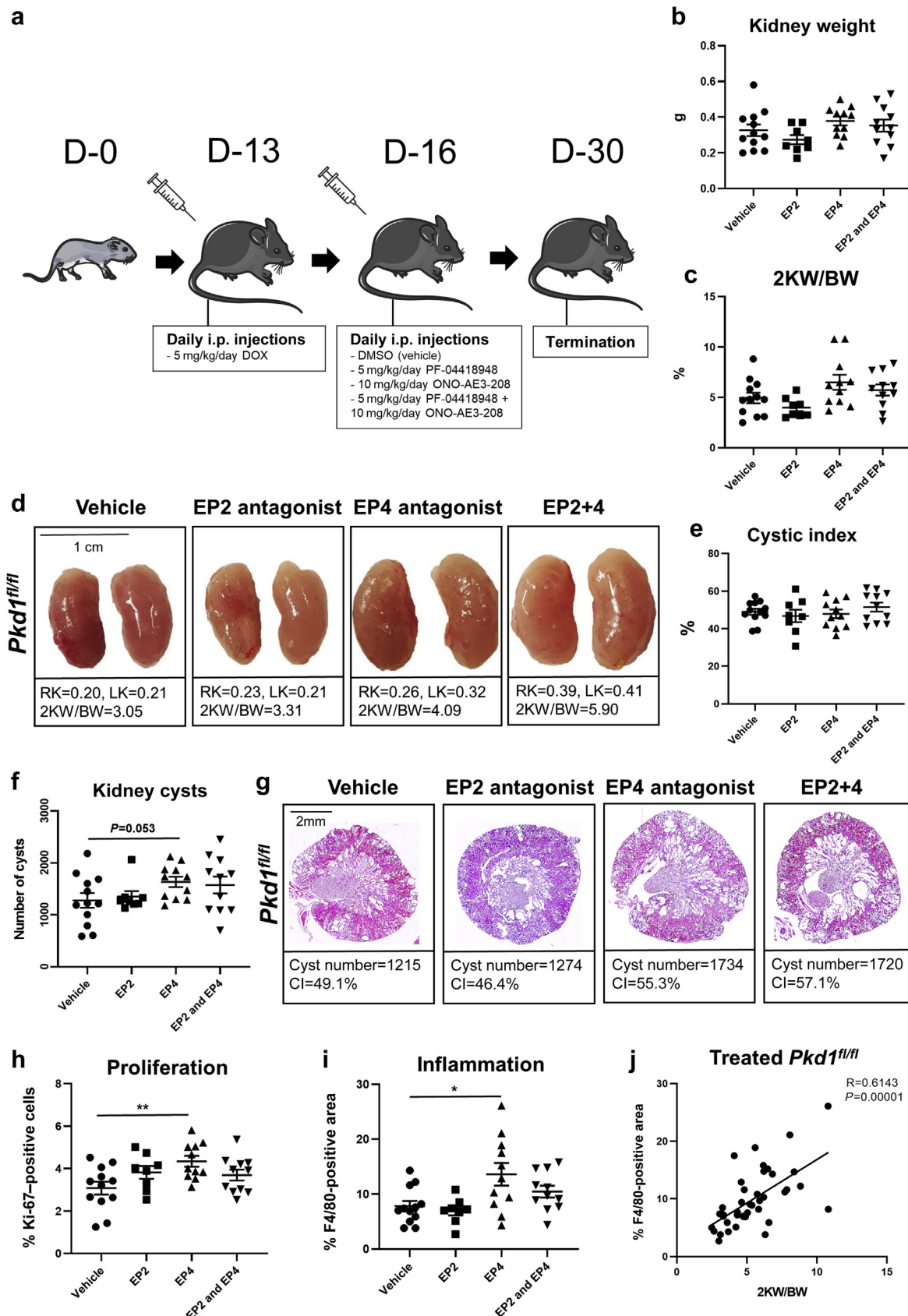


Figure 7 | Administration of an prostaglandin E receptor (EP)4 antagonist increased the cystic phenotype of *Pkd1^{fl/fl}* mice. (a) Outline of experimental strategy. (b) Kidney weight (g), and (c) kidney-to-body weight ratio (2KW/BW) of 30-day-old *Pkd1^{fl/fl}* mice (continued)

receptor expression.^{35,36} The role of EP4 in kidney inflammation has been investigated more extensively than that of EP2. In the unilateral ureteral obstruction (UUO) model, which is characterized by increases in PGE₂, COX-2, EP2, and EP4 mRNA, EP4-null mice developed more interstitial fibrosis and macrophage infiltration compared to wild-type UUO mice.³⁷ Conversely, treating UUO-wild type mice with an EP4 agonist (ONO-4819) reduced interstitial fibrosis and macrophages number.³⁷ A similar effect of a different EP4 agonist (CP-044,519-02) on fibrosis and macrophage infiltration was noted in the subtotal (5/6) nephrectomy model of chronic kidney failure.³⁸ These observations are not restricted to kidney disease models, as EP4-null mice develop greater airway inflammation than their wild-type controls in 3 models of airway inflammation.³⁹ The anti-inflammatory effect of EP4 on macrophages could relate to alternative non-Gs/cAMP pathways such as EP4 receptor-associated protein/ β -arrestin signaling in these cells.⁴⁰

By contrast, the role of EP2 in kidney disease models has not been studied in detail. However, a likely role in the regulation of macrophage maturation has emerged. EP2 expression is upregulated in activated peritoneal macrophages,⁴¹ but EP2-null macrophages or macrophages treated with EP2 antagonist exhibit enhanced maturation *in vitro*; EP2-null mice had higher numbers of mature macrophages circulating and in the peritoneal cavity.⁴² The removal of this restraint on systemic macrophage maturation could have contributed to increased macrophage recruitment in EP2-treated *Pkd1* hypomorphic mice.

Several recent articles have highlighted the role that macrophages could play in modifying disease severity in other murine models of ADPKD.^{43,44} Macrophages have been shown to promote cyst growth by both proliferation-dependent and proliferation-independent mechanisms.⁴⁵ Typically, alternatively activated (M2-like) macrophages have been associated with tubular proliferation, whereas proinflammatory (M1-like) macrophages can lead to cyst expansion through tubular injury.^{45,46} Conversely, the cystic epithelium can play a direct role in stimulating macrophage infiltration (monocyte chemoattractant protein [MCP]-1 secretion) or polarization to M2 phenotypes (L-lactic acid secretion).⁴⁶ Our results add cystic-derived PGE₂ to the emerging epithelial-macrophage axis in ADPKD as both a pro-proliferative and anti-inflammatory mediator. Our *in vivo* results were more complex than anticipated, owing to the opposing effects of EP2 and EP4 on epithelial

proliferation and macrophage infiltration or activation. Of interest, mice treated with EP2 and EP4 antagonists in combination had proliferative rates similar to those of vehicle-treated mice, but they still had more macrophages and a higher cystic index. These results suggest that the direct effects of EP2 and EP4 antagonists in blocking PGE₂-stimulated epithelial cell proliferation (that we observed *in vitro*) were unable to counterbalance the negative effect of increased macrophage infiltration or activation that led to both proliferation and injury. A consistent effect in both models was the increase in F4/80-positive macrophage number (especially M2-like) following EP4 receptor blockade. Our data therefore add to the accumulating evidence that macrophages play a key role in modifying cystogenesis in ADPKD. The complexity of different macrophage subpopulations in healthy and diseased kidney has been reported recently by several groups. Of potential relevance to our findings was the reaccumulation of a “juvenile-like” resident macrophage population (R2b) in pre-cystic kidneys of a cilia mouse mutant (*Ifi88*): R2b macrophages express CD206/Mrc1 and Ym1, classical “M2” markers, and appeared to stimulate cystogenesis in this model.⁴⁷ The role of PGE₂ and particularly EP4 in regulating the accumulation and/or activation of M2 and R2b macrophages in cystic kidneys merits further investigation. It would be interesting to test the ability of EP4 (or EP2) agonists to induce anti-inflammatory effects in this and other PKD models, as has been reported elsewhere.^{37,38} However, we predict that such a test would likely induce direct proliferative effects on cystic epithelial cells.

Our study has some limitations. We only tested the effects of blocking EP2 and EP4 in the earliest phase of disease (PN1–21) coinciding with the peak of cyst formation. Our results therefore do not exclude a role for EP2 or EP4 in the subsequent stages of disease, such as in the late development of fibrosis in this model. Second, the *Pkd1*^{nl/nl} model is an early-onset model with significant cystic disease detectable at birth. We did not test the role of blocking EP2 or EP4 *in utero*, as this could have interfered with embryonic development. A genetic approach would be necessary to test an earlier role for EP2 or EP4 deficiency in the cystic phenotype.

In conclusion, we have shown that PGE₂ induces cyst formation and expansion via activation of EP2 and EP4 receptors through stimulating cell proliferation and decreasing cell apoptosis. Despite the positive effects of EP2 and EP4 antagonists on slowing down cyst growth *in vitro*, the more complex effects of inhibiting EP2 or EP4 *in vivo* resulted in a

Figure 7 | (continued) treated with EP2 or EP4 antagonists. **(d)** Gross morphology of *Pkd1*^{nl/nl} kidneys from mice treated with EP2 or EP4 antagonists. **(e)** Cystic index (%) and **(f)** kidney cysts (number) of *Pkd1*^{nl/nl} kidneys from mice treated with EP2 or EP4 antagonists. **(g)** Representative images of hematoxylin and eosin–stained kidney sections from *Pkd1*^{nl/nl} kidneys from mice treated with EP2 or EP4 antagonists. **(h)** Percentage of Ki-67–positive cells on kidney sections from mice treated with EP2 or EP4 antagonists. **(i)** Percentage of F4/80-positive cells on kidney sections from mice treated with EP2 or EP4 antagonists. **(j)** Correlation between the percentage of F4/80-positive cells and kidney-to-body weight ratio. Values are expressed as mean \pm SEM, $n = 8$ –12 mice per group. * $P < 0.05$; ** $P < 0.01$, compared to vehicle group. Statistical significance was determined using an unpaired *t* test. CI, confidence interval; DMSO, dimethylsulfoxide; LK, left kidney; RK, right kidney. To optimize viewing of this image, please see the online version of this article at www.kidney-international.org.

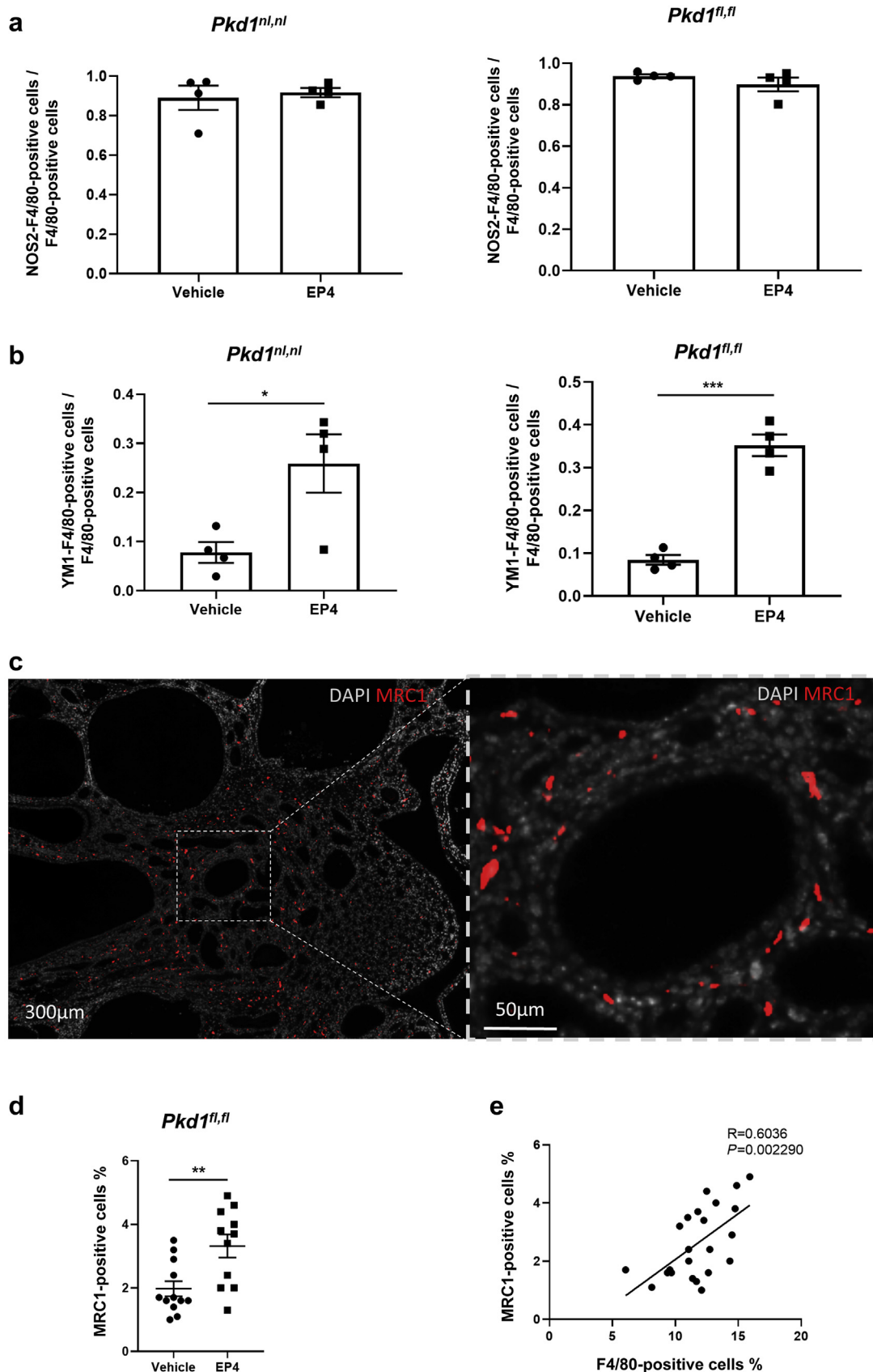


Figure 8 | Macrophage subtypes in prostaglandin E receptor (EP)4 antagonist-treated mice. Fraction of (a) Nos2-F4/80 and (b) Ym1-F4/80 macrophages from *Pkd1^{nl,nl}* (left) and *Pkd1^{fl,fl}* mice (right) in vehicle and EP4 antagonist groups. Values are expressed as (continued)

more severe cystic phenotype *in vivo* due to unexpected proinflammatory effects (Figure 9).

METHODS

Cell lines

MDCK II cells were cultured in Dulbecco's modified Eagle's medium (Gibco, Paisley, UK) supplemented with 10% fetal calf serum (Sigma-Aldrich, Dorset, UK), 50 U/ml penicillin/streptomycin (Lonza, Slough, UK), and 2 mmol/l L-glutamine (Lonza), and maintained at 37 °C in a humidified atmosphere of 5% CO₂. The generation of conditionally immortalized human normal (UCL93) and PKD1 cyst-lining epithelial cells (OX161) has been previously described.^{24,48} In 3D culture, OX161 cells gave rise to predominant cystic (60%) but also simple tubular structures or complex tubulocystic structures. We recloned this line by single-cell dilution to identify clones with a higher ratio (90%) of cysts in 3D culture and chose clone 1 (C1) for further study. Immortalized human cells were cultured in DMEM (Gibco) supplemented with 5% Nu-Serum (Corning, Wilford, UK), 50 U/ml penicillin/streptomycin (Lonza), and 2 mmol/l L-glutamine (Lonza) and maintained at 33 °C in a humidified atmosphere of 5% CO₂.

Experimental animals and study design

All animal experiments were performed under the authority of a UK Home Office license. Hypomorphic *Pkd1*^{nl/nl} harboring an intronic neomycin-cassette in the *Pkd1* gene and their *Pkd1*^{wt/wt} and *Pkd1*^{wt/nl} littermates were sacrificed at different ages from PN1 to PN70 to study the evolution of the disease ($n = 2$ –11 per group).²⁵ *Pax8*^{rtTA-TetO-Cre-Pkd1}^{fl/fl} mice (*Pkd1*^{fl/fl}) were induced using doxycycline (DOX) by daily i.p. injections for 3 days (5mg/kg per day, PN13–15).²⁶ To study the effect of EP2 and EP4 antagonists on disease progression, *Pkd1*^{nl/nl} ($n = 6$ –7) and *Pkd1*^{fl/fl} ($n = 8$ –12) were divided into 4 groups: one vehicle-treated control group; one group treated with 5 mg/kg per day PF-04418948, a selective EP2 antagonist; one group treated with 10 mg/kg per day ONO-AE3-208, a selective EP4 antagonist; and one group treated with 5 mg/kg per day PF-04418948 and 10 mg/kg per day ONO-AE3-208 in combination. *Pkd1*^{nl/nl} mice: from PN1 to PN7, drugs were dissolved in the drinking water and delivered to the pups through the milk, and from PN7 to PN20, drugs were administered by daily i.p. injections. Mice from the vehicle group received daily i.p. injections of dimethylsulfoxide in Kolliphor EL (Sigma-Aldrich). Mice were sacrificed at PN21, corresponding to the peak of the disease. *Pkd1*^{fl/fl} mice: from PN16 to PN29, drugs were administered by daily i.p. injections. Mice from the vehicle group received daily i.p. injections of dimethylsulfoxide in Kolliphor EL. Mice were sacrificed at PN30, corresponding to the peak of the disease.

Cyclic AMP Enzyme-Linked Immunosorbent Assays (ELISAs)

Kidneys were mechanically homogenized in 0.1 M HCl (Acros Organics, Loughborough, UK) using pre-filled Triple-pure zirconium beads (Benchmark Scientific, St Neots, UK) and a microtube homogenizer (Benchmark Scientific) at 4 °C. After centrifugation at $\times 10,000$ g for 10 minutes, cAMP from the supernatant was quantified using an enzyme immunoassay kit (Enzo, Exeter, UK) following manufacturer instructions without acetylation.

Cyclic AMP extracted from cells was quantified using an in-house ELISA we have developed and validated against the commercial ELISA (Supplementary Figure S8E). After 24 hours of starvation, confluent cells were incubated for 30 minutes with 0.25 mmol/l 3-isobutyl-1-methylxanthine (Sigma-Aldrich) and 5 mg/ml lactalbumin hydrolysate (Sigma-Aldrich) prior to incubation with drugs to be tested (Sigma-Aldrich) for 1 hour. Cells were lysed in 0.1 mol/l HCl, and cAMP was measured as follows. ELISA 96-well enzyme immunoassay/radioimmunoassay plates (Costar, Wilford, UK) were coated overnight with 5 µg/ml Goat Anti-Rabbit IgG Antibody (Millipore, Watford, UK) in phosphate buffered saline. After washing the plate with 0.05% Tween 20 in phosphate buffered saline, pH 7.2–7.4, the plates were blocked with 1% bovine serum albumin (Acros-Organics) in phosphate buffered saline, pH 7.2–7.4 for 1 hour at room temperature, followed by additional washes with washing buffer. Competitive reactions to measure cAMP were done by pipetting into wells the same volume of cAMP lysate, neutralizing reagent (Tris-Base 0.1 mol/l; Sigma-Aldrich), rabbit anti-cAMP Antibody (Genscript, Oxford, UK), and cAMP– horseradish peroxidase (Genscript) and incubating the plate for 2 hours at room temperature on a plate shaker. Known concentrations of cAMP (Sigma-Aldrich) diluted in 0.1 mol/l HCl were used to generate a standard curve covering the concentration range 3 to 729 pmol/ml. After extensive washes, the plate was incubated with 3,3',5,5'-tetramethylbenzidine substrate (Thermo Fisher, Paisley, UK) at room temperature for ~20 minutes after which stop solution (2 M sulfuric acid) was added and the absorbance was measured at 450 nm using an ELISA plate reader. Protein concentration was quantified using a detergent compatible protein assay kit (Bio-Rad, Watford, UK) and used to normalize cAMP concentrations.

See the Supplementary Methods for description of other methods used in this study.

Statistical analysis

Data are presented as mean \pm SEM. Statistical analyses were performed with GraphPad Prism (San Diego, CA) software. The degree of significance is denoted as follows: * $P < 0.05$; ** $P < 0.01$; *** $P < 0.001$; **** $P < 0.0001$. The test performed for statistical analysis is indicated in the graph legend.

Figure 8 | (continued) mean \pm SEM, $n = 4$ mice per group with 5 randomly selected regions used for counting. * $P < 0.05$; *** $P < 0.001$, compared to vehicle group. Statistical significance was determined using an unpaired t test. (c) Fluorescent labeling of kidney sections from *Pkd1*^{nl/nl} mice stained with mannose receptor C type 1 (Mrc1; red) and 4',6-diamidino-2-phenylindole (DAPI; gray). The boxed area is expanded in the right image to show the presence of multiple Mrc1-positive macrophages surrounding a medium-sized cyst. (d) Mrc1-positive cells were quantified in *Pkd1*^{fl/fl} mice treated with vehicle and EP4 antagonist. (e) Correlation between the percentage of F4/80-positive cells and MRC1-positive cells present in serial sections from the same animals. Values are expressed as mean \pm SEM, $n = 11$ –12 mice per group. ** $P < 0.01$, compared to vehicle group. Statistical significance was determined using Welch's t test. To optimize viewing of this image, please see the online version of this article at www.kidney-international.org.

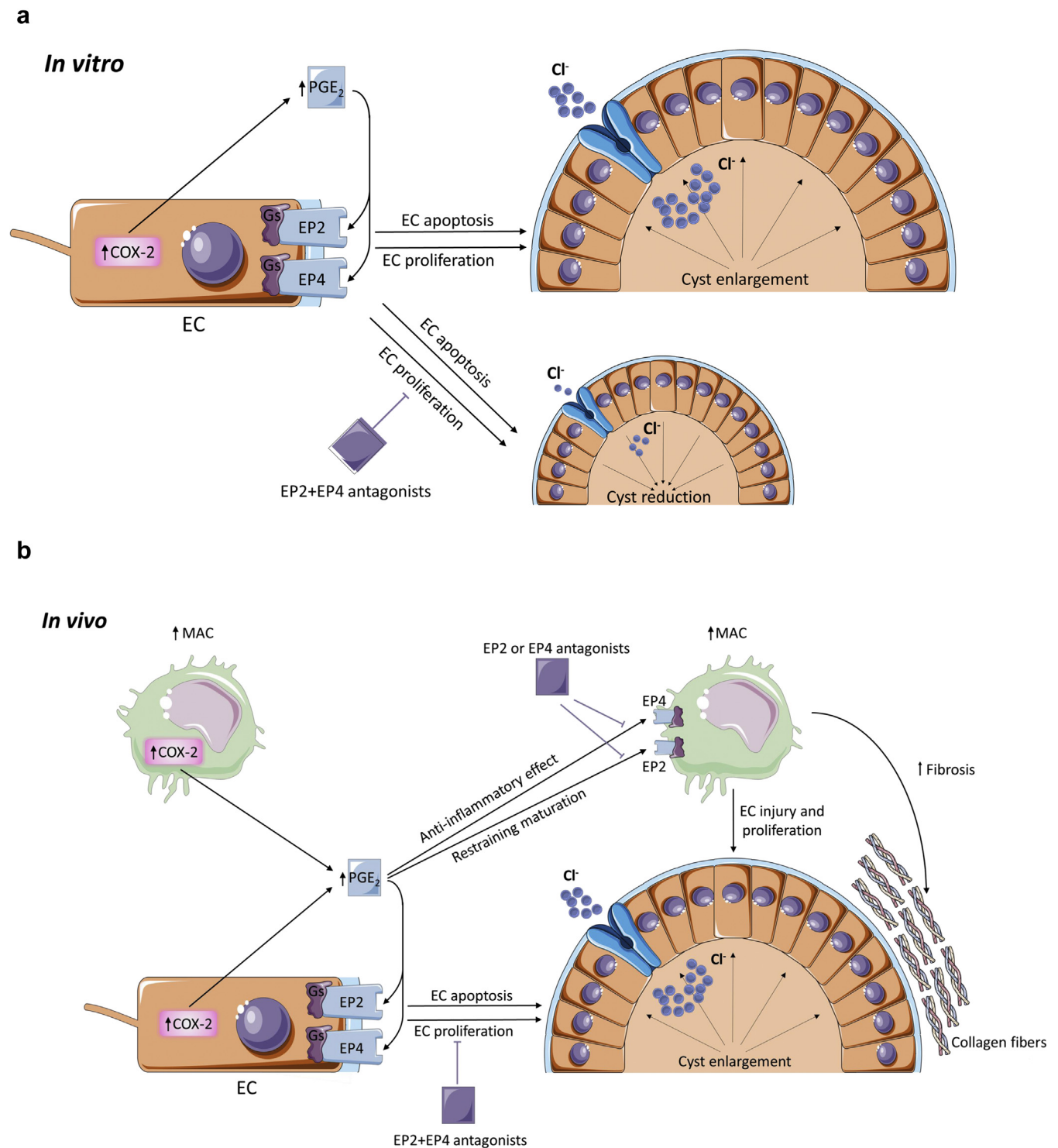


Figure 9 | The likely roles of prostaglandin E receptors (EP)2 and EP4 in autosomal dominant polycystic kidney disease pathogenesis.

(a) *In vitro*, prostaglandin E₂ (PGE₂) enhances cyst growth by stimulating epithelial cell (EC) proliferation, decreasing EC apoptosis, and stimulating chloride (Cl⁻) secretion through EP2- and EP4-mediated cyclic adenosine monophosphate production. (b) *In vivo*, EP2 and EP4 antagonists also induce an increase in macrophage number, which itself leads to an increase in EC injury and proliferation, counteracting the direct effects of EP2 and EP4 on cyst epithelia. The graphical illustration was drawn using the images from Servier Medical Art by Les Laboratoires Servier, with slight modifications (<https://smart.servier.com/>). COX-2, cyclooxygenase-2; MAC, macrophage.

DISCLOSURE

ACMO has received research funding from ONO Pharmaceuticals and has consultancy agreements with Sanofi-Genzyme, Mironid, and Galapagos through the institution. All the other authors declared no competing interests.

ACKNOWLEDGMENTS

We thank Tim Skerry, Fiona Wright, Carl Wright, Jessica Willis, Maya Boudiffa, and Monica Neilan for helpful advice or technical assistance and the late David Huso (Baltimore PKD Centre) for the gift of Pax8-Cre-*Pkd1*^{fl/fl} mice. We gratefully acknowledge the gifts of EP agonists and antagonists from ONO Pharmaceuticals and Pfizer. This project was funded by grants from Kidney Research UK (RP40/2014) and the Sheffield Kidney Research Foundation. FA-A was supported by a PhD studentship from the Libyan government.

SUPPLEMENTARY MATERIAL

[Supplementary File \(PDF\)](#)

Supplementary Methods.

Figure S1. PGE₂ stimulates cell proliferation, decreases cell apoptosis, and induces cAMP formation in MDCK II and OX161-C1 cells.

Figure S2. EP2 and EP4 activation increase cell proliferation and inhibit cell apoptosis in MDCK II cysts.

Figure S3. Early-onset cyst formation in *Pkd1*^{nl/nl} mice.

Figure S4. *Pkd1*^{nl/nl} kidneys are characterised by an increase in proliferating and apoptotic cells.

Figure S5. *Pkd1*^{nl/nl} kidneys are characterized by an increase in interstitial macrophages and fibrosis.

Figure S6. EP1, EP2, EP3, and EP4 gene expression in *Pkd1*^{wt,wt}, *Pkd1*^{wt,nl}, and *Pkd1*^{nl,nl} kidneys from postnatal weeks 2 to 10.

Figure S7. EP4 immuno-localization in 2-week *Pkd1*^{wt,wt} and *Pkd1*^{nl,nl} kidneys.

Figure S8. Additional analysis of *Pkd1*^{nl,nl} mice treated with EP2 and EP4 antagonists.

Figure S9. Segmental origin of cysts in *Pkd1*^{nl,nl} mice treated with EP2 and EP4 antagonists.

Figure S10. Macrophage subtypes in *Pkd1*^{nl,nl} and *Pkd1*^{fl/fl} mice treated with EP4 antagonists.

REFERENCES

- Ong AC, Devuyst O, Knebelmann B, et al. Autosomal dominant polycystic kidney disease: the changing face of clinical management. *Lancet*. 2015;385:1993–2002.
- Grantham JJ, Chapman AB, Torres VE. Volume progression in autosomal dominant polycystic kidney disease: the major factor determining clinical outcomes. *Clin J Am Soc Nephrol*. 2006;1:148–157.
- Lanoix J, D'Agati V, Szabolcs M, et al. Dysregulation of cellular proliferation and apoptosis mediates human autosomal dominant polycystic kidney disease (ADPKD). *Oncogene*. 1996;13:1153–1160.
- Torres VE, Higashihara E, Devuyst O, et al. Effect of tolvaptan in autosomal dominant polycystic kidney disease by CKD stage: results from the TEMPO 3:4 trial. *Clin J Am Soc Nephrol*. 2016;11:803–811.
- Torres VE, Chapman AB, Devuyst O, et al. Tolvaptan in later-stage autosomal dominant polycystic kidney disease. *N Engl J Med*. 2017;377:1930–1942.
- Hanna VS, Hafez EAA. Synopsis of arachidonic acid metabolism: a review. *J Adv Res*. 2018;11:23–32.
- Brock TG, McNish RW, Peters-Golden M. Arachidonic acid is preferentially metabolized by cyclooxygenase-2 to prostacyclin and prostaglandin E2. *J Biol Chem*. 1999;274:11660–11666.
- Vidensky S, Zhang Y, Hand T, et al. Neuronal overexpression of COX-2 results in dominant production of PGE2 and altered fever response. *Neuromolecular Med*. 2003;3:15–28.
- Coleman RA, Smith WL, Narumiya S. International Union of Pharmacology classification of prostanoid receptors: properties, distribution, and structure of the receptors and their subtypes. *Pharmacol Rev*. 1994;46:205–229.
- Breyer MD, Breyer RM. G protein-coupled prostanoid receptors and the kidney. *Annu Rev Physiol*. 2001;63:579–605.
- Hanaoka K, Guggino WB. cAMP regulates cell proliferation and cyst formation in autosomal polycystic kidney disease cells. *J Am Soc Nephrol*. 2000;11:1179–1187.
- Neufeld TK, Douglass D, Grant M, et al. In vitro formation and expansion of cysts derived from human renal cortex epithelial cells. *Kidney Int*. 1992;41:1222–1236.
- Yang B, Sonawane ND, Zhao D, et al. Small-molecule CFTR inhibitors slow cyst growth in polycystic kidney disease. *J Am Soc Nephrol*. 2008;19:1300–1310.
- Anders C, Ashton N, Ranjzad P, et al. Ex vivo modeling of chemical synergy in prenatal kidney cystogenesis. *PLoS One*. 2013;8:e57797.
- Chang MY, Parker E, El Nahas M, et al. Endothelin B receptor blockade accelerates disease progression in a murine model of autosomal dominant polycystic kidney disease. *J Am Soc Nephrol*. 2007;18:560–569.
- Gattone VH 2nd, Wang X, Harris PC, et al. Inhibition of renal cystic disease development and progression by a vasopressin V2 receptor antagonist. *Nat Med*. 2003;9:1323–1326.
- Masyuk TV, Masyuk AI, Torres VE, et al. Octreotide inhibits hepatic cystogenesis in a rodent model of polycystic liver disease by reducing cholangiocyte adenosine 3',5'-cyclic monophosphate. *Gastroenterology*. 2007;132:1104–1116.
- Masyuk TV, Radtke BN, Stroope AJ, et al. Pasireotide is more effective than octreotide in reducing hepatorenal cystogenesis in rodents with polycystic kidney and liver diseases. *Hepatology*. 2013;58:409–421.
- Gardner KD Jr, Burnside JS, Elzinga LW, et al. Cytokines in fluids from polycystic kidneys. *Kidney Int*. 1991;39:718–724.
- Sorensen SS, Glud TK, Sorensen PJ, et al. Change in renal tubular sodium and water handling during progression of polycystic kidney disease: relationship to atrial natriuretic peptide. *Nephrol Dial Transplant*. 1990;5:247–257.
- Elberg G, Elberg D, Lewis TV, et al. EP2 receptor mediates PGE2-induced cystogenesis of human renal epithelial cells. *Am J Physiol Renal Physiol*. 2007;293:F1622–F1632.
- Elberg D, Turman MA, Pullen N, et al. Prostaglandin E2 stimulates cystogenesis through EP4 receptor in IMCD-3 cells. *Prostaglandins Other Lipid Mediat*. 2012;98:11–16.
- Markovic T, Jakopin Z, Dolenc MS, et al. Structural features of subtype-selective EP receptor modulators. *Drug Discov Today*. 2017;22:57–71.
- Streets AJ, Magayr TA, Huang L, et al. Parallel microarray profiling identifies ErbB4 as a determinant of cyst growth in ADPKD and a prognostic biomarker for disease progression. *Am J Physiol Renal Physiol*. 2017;312:F577–F588.
- Lantinga-van Leeuwen IS, Dauwerse JG, Baelde HJ, et al. Lowering of *Pkd1* expression is sufficient to cause polycystic kidney disease. *Hum Mol Genet*. 2004;13:3069–3077.
- Cebotaru L, Liu Q, Yanda MK, et al. Inhibition of histone deacetylase 6 activity reduces cyst growth in polycystic kidney disease. *Kidney Int*. 2016;90:90–99.
- Regan JW, Bailey TJ, Pepperl DJ, et al. Cloning of a novel human prostaglandin receptor with characteristics of the pharmacologically defined EP2 subtype. *Mol Pharmacol*. 1994;46:213–220.
- Bastien L, Sawyer N, Grygorczyk R, et al. Cloning, functional expression, and characterization of the human prostaglandin E2 receptor EP2 subtype. *J Biol Chem*. 1994;269:11873–11877.
- Regan JW, Bailey TJ, Donello JE, et al. Molecular cloning and expression of human EP3 receptors: evidence of three variants with differing carboxyl termini. *Br J Pharmacol*. 1994;112:377–385.
- Funk CD, Furci L, FitzGerald GA, et al. Cloning and expression of a cDNA for the human prostaglandin E receptor EP1 subtype. *J Biol Chem*. 1993;268:26767–26772.
- Huang JL, Woolf AS, Kolatsi-Joannou M, et al. Vascular endothelial growth factor C for polycystic kidney diseases. *J Am Soc Nephrol*. 2016;27:69–77.
- Zhou X, Fan LX, Peters DJ, et al. Therapeutic targeting of BET bromodomain protein, Brd4, delays cyst growth in ADPKD. *Hum Mol Genet*. 2015;24:3982–3993.
- Leonhard WN, Kunnen SJ, Plugge AJ, et al. Inhibition of activin signaling slows progression of polycystic kidney disease. *J Am Soc Nephrol*. 2016;27:3589–3599.

34. Chen L, Zhou X, Fan LX, et al. Macrophage migration inhibitory factor promotes cyst growth in polycystic kidney disease. *J Clin Invest*. 2015;125:2399–2412.
35. Ricciotti E, FitzGerald GA. Prostaglandins and inflammation. *Arterioscler Thromb Vasc Biol*. 2011;31:986–1000.
36. Nakanishi M, Rosenberg DW. Multifaceted roles of PGE₂ in inflammation and cancer. *Semin Immunopathol*. 2013;35:123–137.
37. Nakagawa N, Yuhki K, Kawabe J, et al. The intrinsic prostaglandin E₂-EP₄ system of the renal tubular epithelium limits the development of tubulointerstitial fibrosis in mice. *Kidney Int*. 2012;82:158–171.
38. Vukicevic S, Simic P, Borovecki F, et al. Role of EP₂ and EP₄ receptor-selective agonists of prostaglandin E₂ in acute and chronic kidney failure. *Kidney Int*. 2006;70:1099–1106.
39. Birrell MA, Maher SA, Dekkak B, et al. Anti-inflammatory effects of PGE₂ in the lung: role of the EP₄ receptor subtype. *Thorax*. 2015;70:740–747.
40. Nakatsuji M, Minami M, Seno H, et al. EP₄ receptor-associated protein in macrophages ameliorates colitis and colitis-associated tumorigenesis. *PLoS Genet*. 2015;11:e1005542.
41. Ikegami R, Sugimoto Y, Segi E, et al. The expression of prostaglandin E receptors EP₂ and EP₄ and their different regulation by lipopolysaccharide in C3H/HeN peritoneal macrophages. *J Immunol*. 2001;166:4689–4696.
42. Zaslon Z, Serezani CH, Okunishi K, et al. Prostaglandin E₂ restrains macrophage maturation via E prostanoïd receptor 2/protein kinase A signaling. *Blood*. 2012;119:2358–2367.
43. Karihaloo A, Korashy F, Huen SC, et al. Macrophages promote cyst growth in polycystic kidney disease. *J Am Soc Nephrol*. 2011;22:1809–1814.
44. Swenson-Fields KI, Vivian CJ, Salah SM, et al. Macrophages promote polycystic kidney disease progression. *Kidney Int*. 2013;83:855–864.
45. Cassini MF, Kakade VR, Kurtz E, et al. Mcp1 promotes macrophage-dependent cyst expansion in autosomal dominant polycystic kidney disease. *J Am Soc Nephrol*. 2018;29:2471–2481.
46. Yang Y, Chen M, Zhou J, et al. Interactions between macrophages and cyst-lining epithelial cells promote kidney cyst growth in Pkd1-deficient mice. *J Am Soc Nephrol*. 2018;29:2310–2325.
47. Zimmerman KA, Song CJ, Li Z, et al. Tissue-resident macrophages promote renal cystic disease. *J Am Soc Nephrol*. 2019;30:1841–1856.
48. Parker E, Newby LJ, Sharpe CC, et al. Hyperproliferation of PKD1 cystic cells is induced by insulin-like growth factor-1 activation of the Ras/Raf signalling system. *Kidney Int*. 2007;72:157–165.